COBEM 2023 27TH INTERNATIONAL CONGRESS OF MECHANICAL ENGENEERING

ABCM Brazilian Society of Mechanical Sciences and Engineering
27th ABCM International Congress of Mechanical Engineering
December 04-08, 2023, Florianópolis-SC, Brazil

Vehicle stability using an automotive electronic system: yaw rate, side-slip angle, and roll rate control

Carlos A. Arronte Delgado
Andrei Araujo Felix
Matheus Rotava de Campos Soares
Bruno Augusto Angélico
Diego Colón
Department of Telecommunications and Control Engineering. EPUSP, University of São Paulo, São Paulo, Brazil
carronte94@usp.br
andreifelix@usp.br
matheusrotava2@usp.br
angelico@usp.br
diego@lac.usp.br

Gad Alagia Ripari
Department of Mechanical Engineering. EPUSP, University of São Paulo, São Paulo, Brazil
gadripari@usp.br

Abstract. *This work is part of Brazil's "Rota 2030" program, which aims to encourage R&D in the production of automotive technologies to improve vehicle quality and environmental care. The program also establishes mandatory safety requirements for vehicles produced or imported in Brazil. In line with these goals, the study proposes an electronic control system (ESC) that ensures vehicle stability and passenger safety during maneuvers. The proposed ESC uses a 3DOF vehicle model that reflects the behavior of the side-slip angle, yaw rate, and roll angle and uses control strategies based on nonlinear PID and fuzzy controllers. The combination of these control techniques results in strategies for the actuation of brakes and active dampers to maintain vehicle stability during maneuvers. The study concludes with the design of an ESC that can control the stability of a car in abrupt maneuvers, maintaining critical parameters within a safe range. This work represents a step forward in the production and implementation of a Brazilian-made commercial ESC for vehicle safety, in line with the "Rota 2030" program objectives. It provides an effective and economical solution for improving vehicle stability and safety.*

Keywords: *Rota 2030, automotive, ESC, PID, fuzzy*

1. INTRODUCTION

Automobile accidents are a problem that affects millions of people annually. According to UN reports (UN, 2022), such accidents cause the death of 1.3 million people per year and leave about 50 million seriously injured in the same period of time. For this reason, in September 2020, this organization adopted resolution A/RES/74/299 "Improving global road safety", which proclaims a decade of joint action between the UN and WHO with the aim of reducing by at least 50% the number of deaths and injuries caused by road accidents (WHO, 2021). Parallel to this program, Brazil is developing the "Rota 2030" program which is an instrument implemented by the Federal Government through law no. 13,755 of December 10, 2018, by which tax incentives are granted to companies that invest in research, development, and technological innovation activities. One of the objectives of this program is the implementation of safety measures through assisted driving technologies. As part of the systems to be deployed for the achievement of this objective is the design and implementation of electronic stability controls (ESC) (Ministério da Indústria, 2017).

An ESC system is an active vehicle driving stability assistance and control system that modifies the vehicle's momentum by matching the direction of travel desired by the driver and the vehicle's direction of movement (Chung and Lee, 2015). This system is one of the most important and widely used technologies in vehicle safety and its implementation may include the monitoring and control of the vehicle's lateral and vertical stability (Huang and Chen, 2020).

Many authors and researchers have adopted the theme of active vehicle control through countless strategies. In the case of Cho *et al.* (2008), a Unified Chassis Control (UCC) is implemented by integrating an ESC system that ensures lateral stability through differential braking of each wheel individually, an Active Front Steering (AFS) system, and a Continuous Damping Control (CDC) system in charge of maintaining automotive vertical stability. In the above-mentioned paper, the integration of the ESC system with the AFS ensures that the vehicle achieves the desired yaw in the proposed maneuvers by means of sliding control strategies. On the other hand, the CDC system minimizes the vertical oscillations of the car in case of road disturbances. For the development of this work a bicycle model is chosen and the cornering stiffness of

the car is taken into account. In that paper, the design of the UCC controller was done in Matlab/Simulink and the final simulations were done using CarSim.

In the case of Li *et al.* (2019), was developed an ESC system characterized by individual differential braking on each wheel and the control of an active damper. This combination of elements allows lateral and vertical control of the vehicle while maintaining the yaw and roll parameters in acceptable ranges. In this work, eight degrees of freedom (8-DOF) model is used to simulate the behavior of the vehicle dynamics during maneuvers. A characteristic of this model is that it was built for ME-Wheel type tires (without air), so the model of lateral and longitudinal forces of the vehicle has a great variation with respect to the same models with conventional tires. In that work, the control strategy adopted was the fuzzy PID which was designed using Matlab and validated and tested using CarSim.

Another work that approaches this field is that of Cao *et al.* (2013). In there, two coordinated controllers have the function of maintaining yaw and roll stability based on a prediction model of these variables. The model used is nonlinear and has 3-DOF. Moreover, the tire model used is piece-wise linearized. In that work, coordinated control was tested in CarSim using two maneuvers (slalom and double lane change), in both cases it was managed to keep the parameters in range.

In the case of Yoon *et al.* (2009), a Unified Chassis Control (UCC) is developed to improve vehicle lateral stability and rollover. This system combines the action of an ESC acting on the brakes and thus generating lateral stability, a Roll Over Mitigation Control (ROM) which reduces the possibility of a rollover accident, and a Continuous Damping Control (CDC) in charge of reducing the impact of road disturbances on the vehicle's vertical stability. In that case, a 2-DOF bicycle model is used to simulate the lateral dynamics, and another one of equal degrees of freedom is used to model the vehicle roll. Some works adopt active sway bars to enforce roll control, as in Paes and Colón (2018) and others like Falleiros and Colón (2016) balance human comfort and safety.

Several authors,(Zhao and Zhu, 2018) (Onyeka *et al.*, 2018) (Sang and Chen, 2019) (Wu *et al.*, 2022), have proposed the use of a PID controller in an ESC system. However, not in all cases the yaw rate and side-slip angle are controlled simultaneously.

In the case of the present work, an ESC system is designed based on two PID controllers in charge of maintaining the vehicle's lateral stability and a fuzzy controller responsible for damping the vertical dynamics. For the design of the controllers, a linearized 3-DOF bicycle model is used to reflect the behavior of the lateral velocity (V_y), the yaw rate ($\dot{\psi}$), the roll rate ($\dot{\phi}$) and the roll angle (ϕ) in a maneuver. The control inputs of the system are defined as two moment restoring torques, $\mathbf{M_{lat}}$ and $\mathbf{M_{roll}}$, acting on the vehicle rotation around the z-axis and x-axis, respectively. These torques represent the actuation of the car's ABS differential braking system ($\mathbf{M_{lat}}$) and an active anti-roll bar ($\mathbf{M_{roll}}$). On the other hand, the lateral forces resulting from the maneuver itself are considered as disturbances to the system, and their effect is reduced by using a feedforward stage in the controller design. The obtained controls are tested using two different maneuvers: the fishhook maneuver, and sine with dwell. The objective of the designed ESC is to keep the system variables under control in each maneuver, that is, to minimize the lateral and vertical dynamics of the car and to maintain the traced route. The accomplishment of these objectives protects the car from yaw and roll accidents. The obtained controllers showed a good performance in these maneuvers since they manage to minimize the difference between the trajectory planned by the driver and the real one, the side-slip angle, and the roll angle of the system.

2. MODEL

The model selected for the controller design is based on the 3-DOF linear bicycle model obtained in Zulkarnain *et al.* (2012). This model is commonly used for the design of controllers due to its simplicity. The model obtained reflects the behavior of the state variables described above with respect to the rotation of the steering wheel. A yaw restoring torque ($\mathbf{M_{lat}}$) and a torque applied by an active sway bar ($\mathbf{M_{roll}}$) are considered as controlled inputs of the model. On the other hand, the system's lateral forces (F_yf and F_yr) are considered estimated disturbances. These estimations are performed in the present work by means of Pacejka's Magic Formula. Figure 1 shows the physical representation of this model. The equations of the model are shown in the following subheadings.

2.1 State space model of the system

The system of differential equations describing the dynamics of the system are shown in Eq. (1).

$$\begin{cases} m\dot{V_y} = -m_R h\ddot{\phi} - mV_x\dot{\psi} + F_{yf} + F_{yr}, \\ I_z\ddot{\psi} = -I_{xz}\ddot{\phi} + lfF_{yf} - lrF_{yr} + M_{lat}, \\ I_x\ddot{\phi} = -\dot{V_y}m_R h - \ddot{\psi}I_{xz} - \dot{\psi}m_R hV_x + C_p\dot{\phi} + K_p\phi + \frac{1}{I_x}M_{roll}, \end{cases} \tag{1}$$

where $\mathbf{m}$ is the total vehicle mass in kg, $\mathbf{m_R}$ is the rolling mass of the vehicle in kg, $\mathbf{h}$ is the distance from the rolling mass to the roll axis in m, $\mathbf{I_z}$ defines the moment of inertia of the yaw axis in kgm^2, $\mathbf{I_{xz}}$ represents the moment of inertia in xz-axis in kgm^2, $\mathbf{I_x}$ is the moment of inertia of the roll axis expressed in kgm^2, $\mathbf{L_p}$ is the negative coefficient of roll

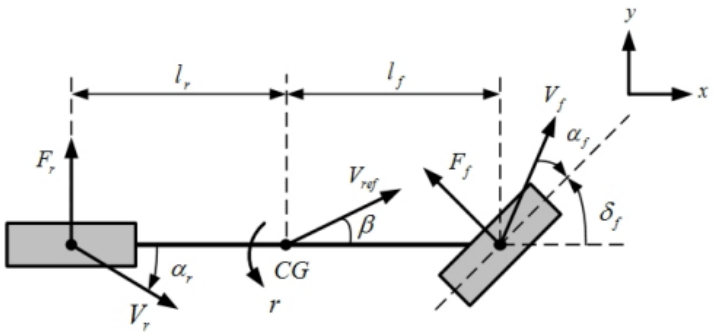

Figure 1: Bicycle model of a vehicle.Taken of Kahraman *et al.* (2020)

damping in Nm/(rad·s) and $\mathbf{L_f}$ is the coefficient of roll stiffness in Nm/rad. With these equations, the state space matrices of the system can be formed as in Eq. (2).

$$\begin{cases} E\dot{x} + Fx = G\begin{bmatrix} M_{lat} \\ M_{roll} \end{bmatrix} + H\begin{bmatrix} F_{yf} \\ F_{yr} \end{bmatrix} \\ y = Cx + Du \end{cases} \tag{2}$$

where:

$$E = \begin{bmatrix} m & 0 & m_R \cdot h & 0 \\ 0 & Iz & Ixz & 0 \\ m_R \cdot h & Ixz & Ix & 0 \\ 0 & 0 & 0 & 1 \end{bmatrix} \qquad F = \begin{bmatrix} 0 & m \cdot u_0 & 0 & 0 \\ 0 & 0 & 0 & 0 \\ 0 & m_R \cdot h \cdot u_0 & -Lp & -Lf \\ 0 & 0 & -1 & 0 \end{bmatrix} \tag{3}$$

$$G = \begin{bmatrix} 0 & 1 & 0 & 0 \\ 0 & 0 & -1/I_x & 0 \end{bmatrix}^T \qquad H = \begin{bmatrix} 1 & 1 \\ l_f & -l_r \\ 0 & 0 \\ 0 & 0 \end{bmatrix} \tag{4}$$

The dynamics of the vehicle's lateral forces in relation to the steering angle are obtained by means of Pacejka's Magic Formula (PMF) (Pacejka, 2012). The lateral force's dynamic is split into two pieces for better comprehension. Equations (5), (6), (7), and (8) show the expressions for the calculation of these forces.

- Front lateral force (F_{yf}) estimation:

$$\phi_{yf} = (1 - E_y)(\alpha_f + S_{hy}) + (E_y/B_y)\tan^{-1}(B_y(\alpha_f + S_{hy})) \tag{5}$$

$$F_{yf} = D_{yf} \cdot \sin(C_y \cdot \tan^{-1}(B_y \cdot \phi_{yf})) + S_{vy} \tag{6}$$

- Rear lateral force (F_{yf}) estimation:

$$\phi_{yr} = (1 - E_y)(\alpha_r + S_{hy}) + (E_y/B_y)\tan^{-1}(B_y(\alpha_r + S_{hy})) \tag{7}$$

$$F_{yr} = D_{yr} \cdot \sin(C_y \cdot \tan^{-1}(B_y \cdot \phi_{yr})) + S_{vy}; \tag{8}$$

where $\alpha_\mathbf{f}$ and $\alpha_\mathbf{r}$ are the front and rear steer of wheels respectively in degrees, $\phi_{\mathbf{yf}}$ and $\phi_{\mathbf{yr}}$ are the maneuver slip ratio concerning the front and rear axle respectively in deg/s, $\mathbf{B_y}$ are the tire stiffness factor, $\mathbf{C_y}$ are the shape factor of the curve, $\mathbf{D_{yf}}$ and $\mathbf{D_{yr}}$ are the peak factor concerning the front and rear axle respectively, $\mathbf{E_y}$ is the wheel curvature factor, $\mathbf{S_{hy}}$ is the car horizontal shift in m, $\mathbf{S_{vy}}$ are the car vertical shift in m. Finally, the vector of lateral forces in Newtons can be expressed like in Eq. (9):

$$Fy = \begin{bmatrix} F_{yf} & F_{yr} \end{bmatrix} \tag{9}$$

The calculation of the front and rear wheel steer as function of the steering wheel steer can be calculated by Eq. (10) and Eq. (11), respectively:

$$\alpha_f = (\delta_f - \frac{v + l_f \cdot \dot{\psi}}{u_0}) \cdot 180/\pi, \tag{10}$$

$$\alpha_r = (-\frac{v - l_r \cdot \dot{\psi}}{u_0}) \cdot 180/\pi \tag{11}$$

where $\delta_\mathbf{f}$ is the steering angle in degrees of the front wheels due to the maneuver, v is the lateral velocity in m/s of the vehicle in the turn, $\mathbf{l_f}$ and $\mathbf{l_r}$ are the distances from the center of gravity (CG) to the front and rear axle respectively in meters, and $\mathbf{u_0}$ is the longitudinal velocity in m/s of the vehicle and is considered as a constant.

3. CONTROL DESIGN

The designed ESC system consists of two independent controllers: one dedicated to minimizing the effect of the car's lateral dynamics and the other one to avoid vehicle rollover due to abrupt maneuvers. These controllers individually calculate the control action on the corresponding parameters and act in unison on the system. These controllers are described in detail in the following sub-sections.

3.1 Lateral dynamic control

This controller is based on the action of two independent PID controllers that keep the side-slip angle (β) and yaw rate ($\dot{\psi}$) caused by the steering wheel turns at reasonable levels. This type of classical controller has the structure $U(s) = (K_p + K_i\frac{1}{s} + K_d \cdot s)e(s)$. The resulting total control action is a restoring torque $\mathbf{M_{lat}}$. This controller will be active only when the controlled parameters are out of the defined range, the rest of the time it will be deactivated which contributes to the decrease of the total control effort. Figure 2 shows the implementation of this controller in Matlab.

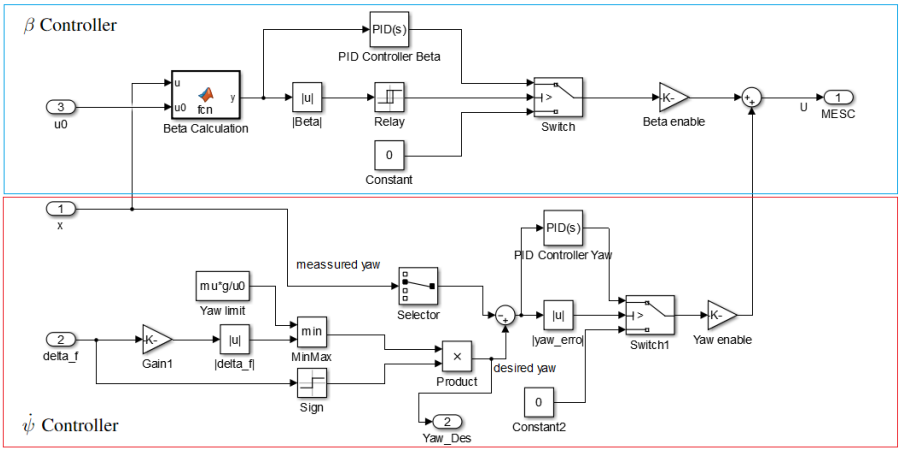

Figure 2: Lateral control implementation in Matlab/Simulink.

3.1.1 Side-slip angle (β) control design

In vehicle dynamics, the side-slip angle is the angle between the direction in which a wheel is pointing and the direction in which it is actually traveling. The relationship between these velocities is expressed in Eq. (12). This slip angle results in a force, the cornering force, which is in the plane of the contact patch and perpendicular to the intersection of the contact patch and the mid-plane of the wheel. This cornering force increases approximately linearly for the first few degrees of slip angle, then increases non-linearly to a maximum before beginning to decrease (Grip *et al.*, 2009). The PID control designed at this stage has the objective of minimizing the side-slip angle since a high value of this parameter indicates a high lateral speed and, therefore, a bigger risk of vehicle flip over. Equation (13) can then be considered as the first control target:

$$\beta = tan^{-1}(\frac{V_y}{V_x}) \tag{12}$$

A hysteresis stage is used to satisfy this criterion with $\pm\beta_{lim}$ as the upper and lower bands.

$$\beta \leq \beta_{lim} \tag{13}$$

3.1.2 Yaw rate ($\dot{\psi}$) control design

The yaw rate is the rate of change of the vehicle's heading angle, measured in degrees/second of rotation about a vertical axis through the vehicle's center of gravity. A high yaw rate implies abrupt changes in the lateral speed of the vehicle which may result in the vehicle leaving the road, colliding with other road users, or rolling off. In this work, it is intended that the yaw rate performs the tracking of a desired reference ($\dot{\psi}_{\mathbf{D}}$). The objective of the control is then the minimization of the difference between $\dot{\psi}_{\mathbf{D}}$ and $\dot{\psi}$. Equation (14) gives away the second control objective:

$$|\dot{\psi} - \dot{\psi}_D| \leq \dot{\psi}_{lim}, \tag{14}$$

To find the limits of $\dot{\psi}$ it is necessary to define its relation to the steering angle as shown in Eq. (15) (see MLA (2022)):

$$\frac{\dot{\psi}}{\delta_f} = \frac{u_0/R}{L/R + K_{us} a_y} \tag{15}$$

where $\mathbf{L}$ is the distance between car axles in m, $\mathbf{R}$ represents the sub steering coefficient, $\mathbf{a_y}$ is the lateral acceleration in m/s^2 and $\mathbf{K_{us}}$ is the car under-steer coefficient. After defining Eq. (16) and substituting it in Eq. (15), the first control limit for the yaw rate is presented in Eq. (17):

$$a_y = \frac{u_0^2}{R} \tag{16}$$

$$\dot{\psi} = \frac{u_0}{L + K_{us} u_0^2} \delta_f = G_{\dot{\psi}} \delta_f \tag{17}$$

On the other hand, the $\mathbf{G}_{\dot{\psi}}$ equation has a natural saturation as shown in Eq. (18):

$$m a_y < \mu m g \rightarrow a_y < \mu g \rightarrow \dot{\psi} < \frac{\mu g}{u_0} \tag{18}$$

The variable μ is the road's friction coefficient and $\mathbf{g}$ is the gravity acceleration. The desired yaw rate error limits are then defined as in Eq. (19):

$$\dot{\psi}_D = \min\left(\left| \frac{\mu g}{u_0} \right|, \left| G_{\dot{\psi}} \delta_f \right| \right) \cdot \text{sign}(\delta_f) \tag{19}$$

3.2 Control of vertical dynamics (ϕ and $\dot{\phi}$)

In this case, a fuzzy controller is designed and implemented to drive the vehicle's roll angle during the maneuver. This controller has three stages: fuzzification, rule evaluation, and defuzzification. In the first stage, the values of roll angle and roll rate are taken and converted into fuzzy values, then the value and fuzzy variables of the output $\mathbf{M_{roll}}$ are calculated according to the values adopted for roll and roll rate in the previous stage. Finally, the fuzzy value of $\mathbf{M_{roll}}$ is converted to a torque signal and passed to the plant. Figure 3a shows the implementation of this controller in Matlab and Fig. 3 shows the configuration screens of the fuzzy controller by the Mandami method in Matlab/Simulink. It should be noted that in the design of this controller, the vector of lateral forces [$\mathbf{Fyf}$, $\mathbf{F_{yr}}$] is considered a predominant deterministic perturbation in the system. To correct the action of these disturbances, a feedforward stage to the controller is designed for each lateral force.

4. SIMULATIONS

The system simulations are performed using Matlab/Simulink. The following maneuvers are used for this purpose.

4.1 Test maneuvers

For the testing of the controllers, two maneuvers are selected to be performed both in Simulink: the Fishhook and the Sine With Dwell maneuvers. The purpose of these maneuvers is to show the behavior of the car parameters in situations that compromise vehicle safety. These maneuvers are briefly described below. Figures 4a and 4b shows the steering angle plots for both maneuvers.

4.1.1 Fishhook maneuver

The Fishhook maneuver uses steering inputs that approximate those of a panicked driver in an effort to regain lane position after veering off the roadway and onto the curb. NHTSA has often described it as a road edge recovery maneuver. As pointed out by some commenters, it is performed on a smooth pavement rather than at a road edge drop-off, but its rapid steering input followed by an over-correction is representative of a general loss of control situation. The original version of this test was developed by Toyota, and Nissan and Honda subsequently proposed variations (Boyd, 2005).

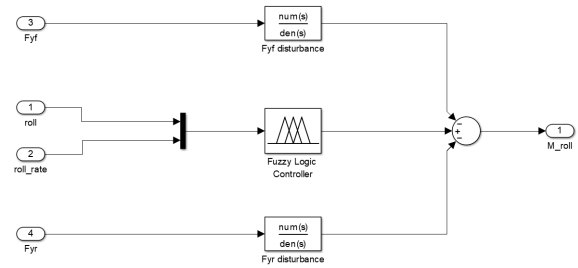

(a) Vertical control implementation in Matlab/Simulink

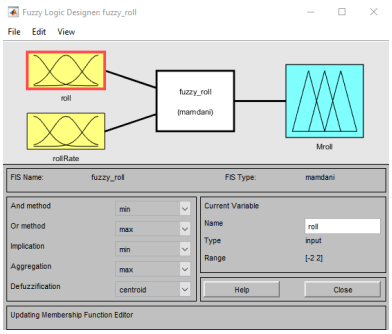

(b) General configuration of 2-input, 1-output fuzzy controller

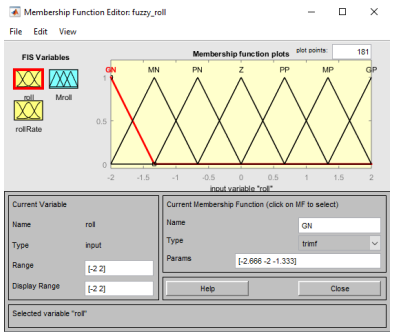

(c) Roll membership functions

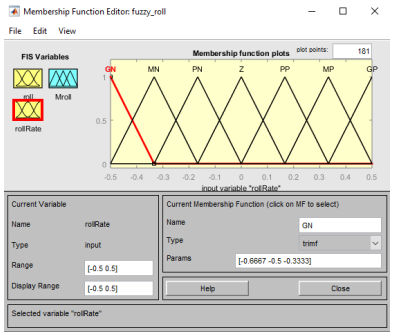

(d) Roll rate membership functions

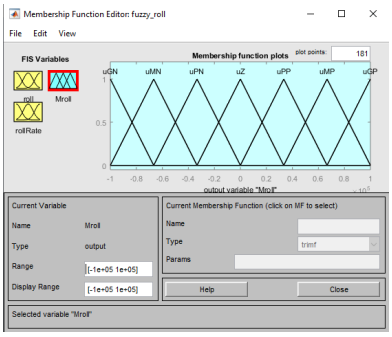

(e) M_{roll} output membership functions

Figure 3: Configuration of the fuzzy controller by the Mandami method in Matlab/Simulink

4.1.2 Sine With Dwell maneuver

The sine with dwell test is based on the test method specified in regulations USA FMVSS 126 and UN/ECE Regulation No. 13-H. This is a method for comparing computer simulation results from a vehicle mathematical model to test data measured for an existing vehicle undergoing sine with dwell tests that are typically used to evaluate the performance of an electronic stability control (ESC) system. The comparison is made for the purpose of validating the simulation tool for this type of test when applied to variants of the tested vehicle (ISO 19365:2016, en).

5. RESULTS

5.1 The Fishhook maneuver's results

Figures 5a and 5b show the behavior of the side-slip angle when performing the Fishhook maneuver with and without control, respectively. Here it can be seen a significant reduction of this parameter, which denotes an effective control of this one. On the other hand, Fig. 6a and Fig. 6b show how the car manages to follow a desired yaw trajectory once this parameter is controlled. It can also be seen in Fig. 7a and Fig. 7b how the fuzzy control reduces the vertical dynamics

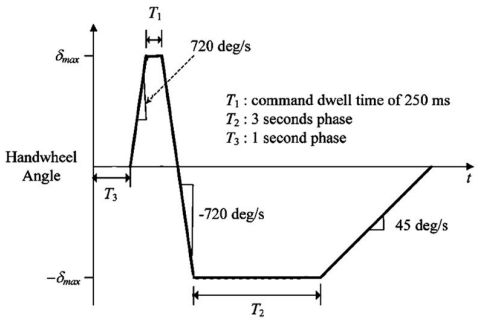

(a) Fishhook maneuver. Taken from Marzbanrad *et al.* (2015).

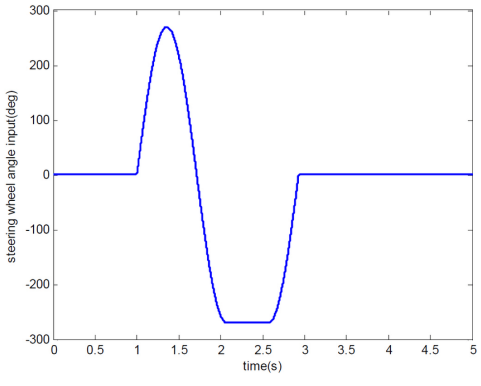

(b) Sine With Dwell Maneuver. Taken fom Ren *et al.* (2014).

Figure 4: Performed test maneuvers

of the car in the maneuver. Finally, Fig. 8 shows the controller efforts exerted during the maneuver. In general, it can be stated that a car with the characteristics of the selected one, would not have passed this test without the proposed control.

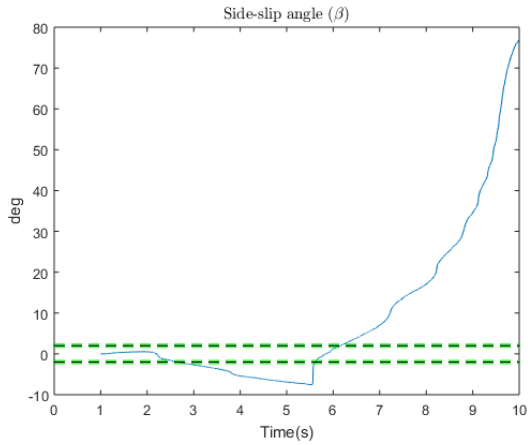

(a) Behavior of the side-slip angle in the Fishhook maneuver in an uncontrolled car.

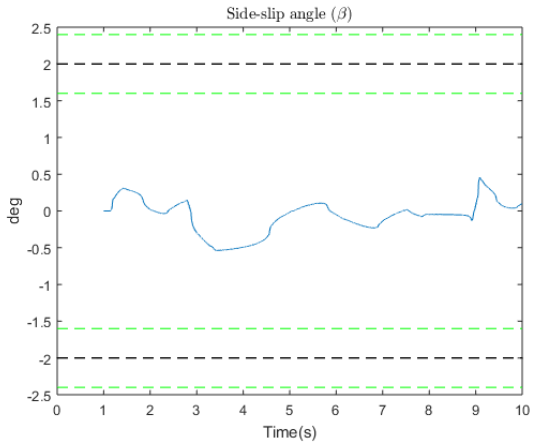

(b) Behavior of the side-slip angle in the Fishhook maneuver in a controlled car.

Figure 5: Behavior of the side-slip angle in the Fishhook maneuver

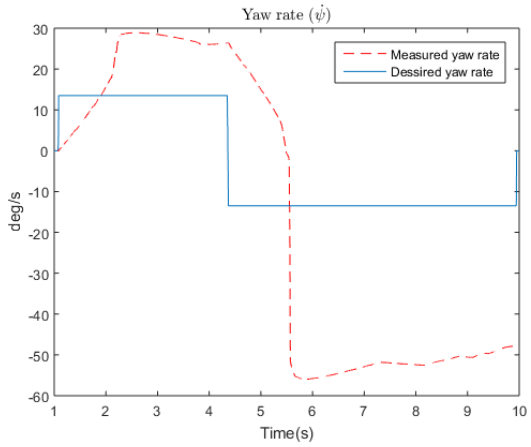

(a) Behavior of the yaw rate in the Fishhook maneuver in an uncontrolled car.

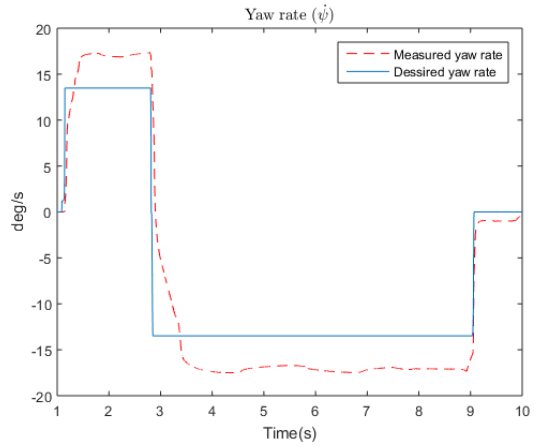

(b) Behavior of the yaw rate in the Fishhook maneuver in a controlled car.

Figure 6: Behavior of the yaw rate in the Fishhook maneuver

5.2 The Sine with Dwell maneuver's results

In this maneuver, similar results to those shown in the previous subsection are observed. On the one hand, Fig. 9a and Fig. 9b show the behavior of the side-slip angle with and without control respectively, demonstrating a strong influence of the controller on the decrease of this parameter. On the other hand, Fig. 10a and Fig. 10b show that the vehicle with the proposed control is able to reduce the difference between the desired path and the actual path traveled. Figures 11a and 11b show the decrease in roll angle and roll rate along the maneuver caused by the proposed fuzzy control. Finally, Fig. 12 shows the effort of the proposed controllers for the horizontal and vertical dynamics.

6. CONCLUSIONS

In the present work, an ESC system is designed with the objective of maintaining in range the main parameters of the horizontal (side-slip angle and yaw rate) and vertical (roll angle and roll rate) vehicle dynamics. This work demonstrates that this controller can keep the car stable in two certified maneuvers that demonstrate a driver's behavior in real situations. The obtained system constitutes an easy-to-implement and low-cost solution for improving vehicle safety as part of the "Rota 2030" program.

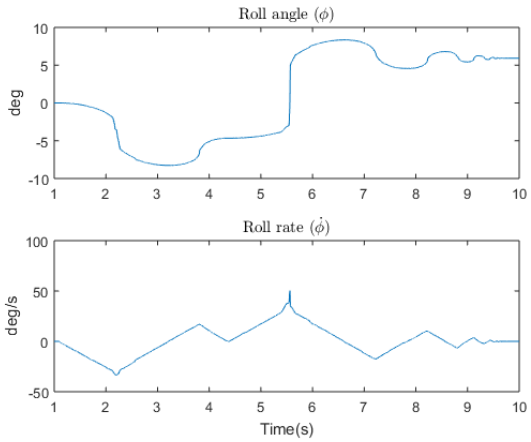

(a) Behavior of the roll and roll rate in the Fishhook maneuver in an uncontrolled car.

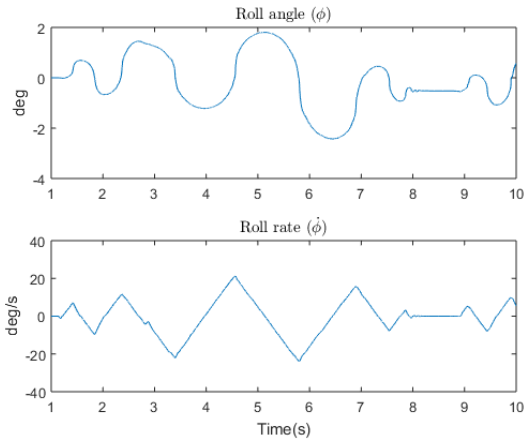

(b) Behavior of the roll and roll rate in the Fishhook maneuver in an uncontrolled car.

Figure 7: Behavior of the roll and roll rate in the Fishhook maneuver

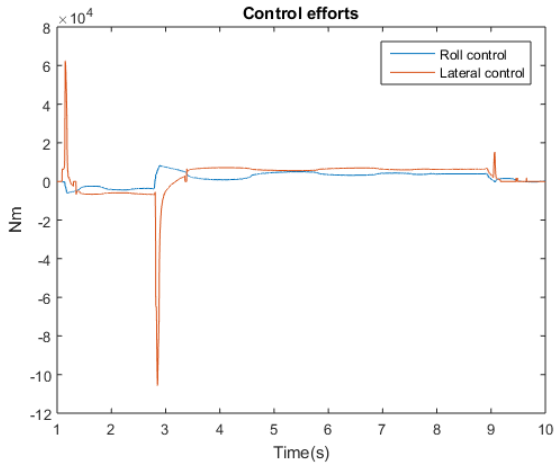

Figure 8: Controller efforts

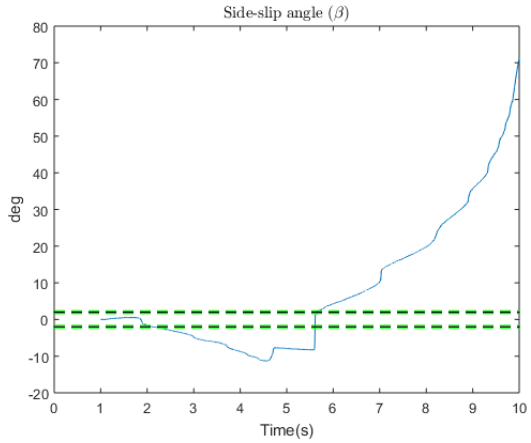

(a) Behavior of the side-slip angle in the Sine width Dwell maneuver in an uncontrolled car.

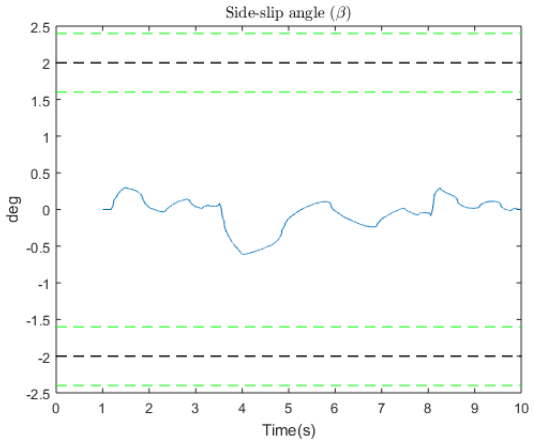

(b) Behavior of the side-slip angle in the Sine width Dwell maneuver in a controlled car.

Figure 9: Behavior of the side-slip angle in the Sine with Dwell maneuver.

7. ACKNOWLEDGEMENTS

Authors would like to thank Fundação de Desenvolvimento da Pesquisa – Fundep Rota 2030 - Linha V, for the Grants SUSP-EST - *Sistema de Suspensão Semi-Ativa para Controle Avançado de Estabilidade* and SEGURAUTO - *Projeto e*

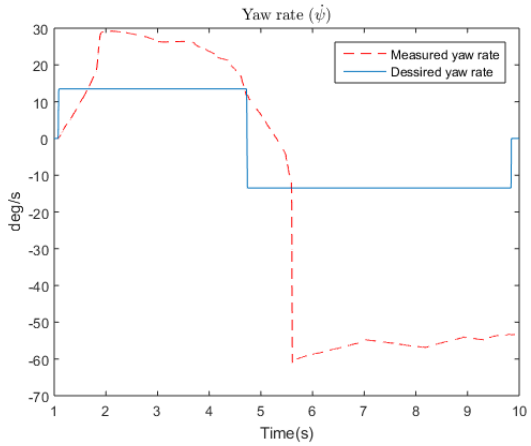

(a) Behavior of the yaw rate in the Sine width Dwell maneuver in an uncontrolled car.

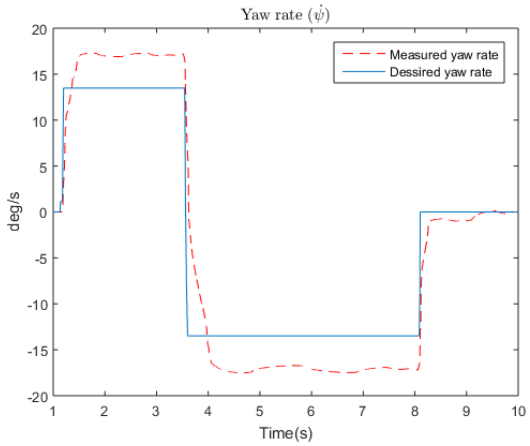

(b) Behavior of the yaw rate in the Sine width Dwell maneuver in a controlled car.

Figure 10: Behavior of the yaw rate in the Sine width Dwell maneuver.

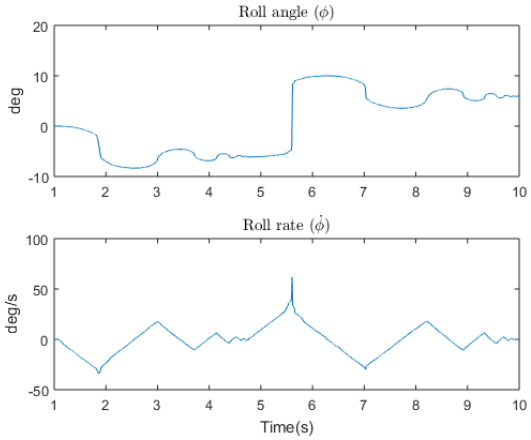

(a) Behavior of the roll and roll rate in the Sine width Dwell maneuver in an uncontrolled car.

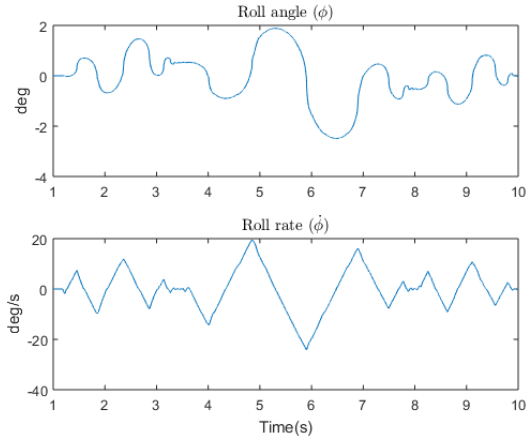

(b) Behavior of the roll and roll rate in the Sine width Dwell maneuver in a controlled car.

Figure 11: Behavior of the roll and roll rate in the Sine width Dwell maneuver.

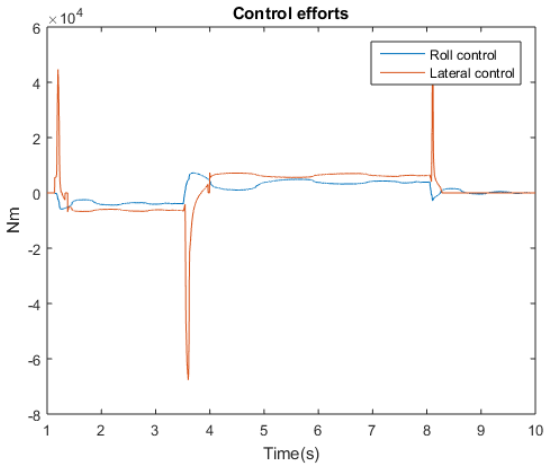

Figure 12: Controller efforts

Desenvolvimento Integrado de Funções de Segurança Assistida ao Condutor e Ambiente para Veículos Autônomos. This study was financed in part by the Coordenação de Aperfeiçoamento de Pessoal de Nível Superior - Brasil (CAPES) - Finance Code 001.

8. REFERENCES

Boyd, P.L., 2005. "Nhtsa's ncap rollover resistance rating system". *19th International Technical Conference on the Enhanced Safety of Vehicles (ESV)*, Vol. 05-0450.

Cao, J., n Jing, L., Guo, K. and Yu, F., 2013. "Study on integrated control of vehicle yaw and rollover stability using nonlinear prediction model". *Mathematical Problems in Engineering*, Vol. 2013, p. 15.

Cho, W., Yoon, J., Kimb, J., Hur, J. and Yi, K., 2008. "An investigation into unified chassis control scheme for optimised vehicle stability and manoeuvrability". *Vehicle System Dynamics*, Vol. 46, pp. 87–105.

Chung, S. and Lee, H., 2015. "Estimating desired yaw rate and control strategy analysis on developed air esc system for performance evaluation". *2015 15th International Conference on Control, Automation and Systems (lCCAS 2015)*.

Falleiros, M.F. and Colón, D., 2016. "Lqg/ltr robust active suspension control applied on a nonlinear half-vehicle model". In *Proceedingd of the CBA 2016*.

Grip, H., Imsland, L., Johansen, T., Kalkkuhl, J. and Suissa, A., 2009. "Vehicle sideslip estimation design, implementation, and experimental validation." *IEEE Control Systems Magazine*, Vol. 29, pp. 36–52.

Huang, Y. and Chen, Y., 2020. "Vehicle lateral stability control based on shiftable stability regions and dynamic margins". *IEEE TRANSACTIONS ON VEHICULAR TECHNOLOGY*, Vol. 69.

ISO 19365:2016(en), 2016. "Passenger cars — Validation of vehicle dynamic simulation — Sine with dwell stability control testing". Standard, International Organization for Standardization, Geneva, CH.

Kahraman, K., Senturk, M., Emirler, M.T., Uygan, I.M.C., Aksun-Guvenc, B., Guvenc, L. and Efendioglu, B., 2020. "Yaw stability control system development and implementation for a fully electric vehicle". *arXiv preprint arXiv:2012.04719*.

Li, H., Zhao, Y., Lin, F. and Xu, H., 2019. "Integrated yaw and rollover stability control of an offroad vehicle with mechanical elastic wheel". *JOURNAL OF VIBROENGINEERING*, Vol. 20.

Marzbanrad, J., Soleimani, G., Mahmoodi-k, M. and Rabiee, A.H., 2015. "Development of fuzzy anti-roll bar controller for improving vehicle stability". Vol. 17, pp. 3856–3864.

Ministério da Indústria, C.E.e.S., 2017. *Rota 2030: Propostas do Governo para uma nova política industrial automotiva. (E-book)*. Ministério da Indústria, Comércio Exterior e Serviços, Brasilia.

MLA, 2022. " CONTROLE DE ESTABILIDADE: MODELAGEM DO SISTEMA DINÂMICO works cited: Electronic sources (web publications)". Youtube, Universidade de Brasilia, https://www.youtube.com/watch?v=jzV82SKc9JA. Accessed 04 Apr 2022.

Onyeka, E., Chidiebere, M., Echezona, E. and Hope, E., 2018. "Simulation performance of antilock braking system under different drag coefficients". *IRJAES*, Vol. 3, pp. 246–251.

Pacejka, H.B., 2012. "Chapter 11 - motorcycle dynamics". In H.B. Pacejka, ed., *Tire and Vehicle Dynamics (Third Edition)*, Butterworth-Heinemann, Oxford, pp. 505–565. Third edition edition. ISBN 978-0-08-097016-5. doi:https://doi.org/10.1016/B978-0-08-097016-5.00011-5. URL `https://www.sciencedirect.com/science/article/pii/B9780080970165000115`.

Paes, J.H. and Colón, D., 2018. "Comparison between passive and active flexible anti-roll bars modelles by finite element method on prevention of vehicle rollovers". In *Proceedings of the CBA 2018*.

Ren, H., Shim, T., Ryu, J. and Chen, S., 2014. "Development of effective bicycle model for wide ranges of vehicle operations". *SAE Technical Papers*, Vol. 1. doi:10.4271/2014-01-0841.

Sang, N. and Chen, L., 2019. "Design of an active front steering system for a vehicle using an active disturbance rejection control method". *Science Progress*, pp. 246–251.

UN, 2022. "Accidentes viales: "una epidemia silenciosa y ambulante" que mata a 1,3 millones de personas por año (web publications)". https://news.un.org/es/story/2022/06/1511112. Accessed 06 Jun 2023.

WHO, 2021. "Decade of action for road safety 2021-2030 (web publications)". https://www.who.int/teams/social-determinants-of-health/safety-and-mobility/decade-of-action-for-road-safety-2021-2030/. Accessed 06 Jun 2023.

Wu, Z., Zhang, X., Kang, C. and Zong, G., 2022. "Can pid make the electronic stability program more effective?" *Research on Co-simulation of Electronic Stability Program, CEUR-WS*, Vol. 3150, p. 6.

Yoon, J., Cho, W., Koo, B. and Yi, K., 2009. "Unified chassis control for rollover prevention and lateral stability". *IEEE TRANSACTIONS ON VEHICULAR TECHNOLOGY*, Vol. 58, No. 2.

Zhao, S. and Zhu, L., 2018. "Cruise control system based on joint simulation of carsim and simulink". *OALib Journal*, Vol. 5.

Zulkarnain, N., Imaduddin, F., Zamzuri, H. and Mazlan, S.A., 2012. "Application of an active anti-roll bar system for enhancing vehicle ride and handling". *2012 IEEE Colloquium on Humanities, Science and Engineering Research (CHUSER 2012), December 3-4, 2012, Kota Kinabalu, Sabah, Malaysia*.

9. RESPONSIBILITY NOTICE

The authors are solely responsible for the printed material included in this paper.